Biogeochemistry (2012) 109:233–252
DOI 10.1007/s10533-011-9623-x

Sediment-water fluxes of dissolved inorganic carbon, O_2, nutrients, and N_2 from the hypoxic region of the Louisiana continental shelf

John C. Lehrter · David L. Beddick Jr. · Richard Devereux · Diane F. Yates · Michael C. Murrell

Received: 4 December 2009 / Accepted: 14 July 2011 / Published online: 29 July 2011

Abstract Globally, hypoxic areas (<63 mmol O_2 m^{-3}) in coastal waters are increasing in number and spatial extent. One of the largest coastal hypoxic regions has been observed during the summer in the bottom-water of the Louisiana continental shelf. The shelf receives the sediments, organic matter, and nutrients exported from the Mississippi River watershed, and much of this material is ultimately deposited to the sea floor. Hence, quantifying the rates of sediment-water dissolved inorganic carbon (DIC), oxygen (O_2), and nutrient fluxes is important for understanding how these processes relate to the development and maintenance of hypoxia. In this study, the sediment-water fluxes of DIC, O_2, nutrients, and N_2 (denitrification) were measured on the Louisiana shelf during six cruises from 2005 to 2007. On each cruise, three to four sites were occupied in or directly adjacent to the region of the shelf that experiences hypoxia. DIC fluxes, a proxy for total sediment respiration, ranged from 7.9 to 21.4 mmol m^{-2} day^{-1} but did not vary significantly either spatially or as a function of bottom-water O_2 concentration. Overall, sediment respiration and nutrient flux rates were small in comparison to water-column respiration and phytoplankton nutrient demand. Nitrate fluxes were correlated with bottom-water O_2 concentrations ($r = 0.69$), and there was evidence that decreasing O_2 concentrations inhibited coupled nitrification-denitrification. Denitrification rates averaged 1.4 mmol N m^{-2} day^{-1}. Scaled to the area of the shelf, the denitrification sink represented approximately 39% of the N load from the Mississippi River watershed. The sediment-water fluxes reported from this study add substantial information on the spatial and temporal patterns in carbon, O_2, and nutrient cycling available for the Louisiana continental shelf and, thus, improve the understanding of this system.

Keywords Sediment-water DIC · O_2 and nutrient flux · Denitrification · Hypoxia · LOUISIANA shelf

J. C. Lehrter (✉) · D. L. Beddick Jr. · R. Devereux · D. F. Yates · M. C. Murrell
Gulf Ecology Division, US EPA, NHEERL, 1 Sabine Island Drive, Gulf Breeze, FL 32561, USA
e-mail: lehrter.john@epa.gov

Introduction

Hypoxic areas in coastal waters have increased globally in number and spatial extent (Diaz and Rosenberg 2008). The seasonally hypoxic region of the Louisiana shelf is typical of the global distribution of hypoxic regions, being located adjacent to a watershed highly altered by human activities and discharging large nutrient loads. In combination with the eutrophication, the Louisiana shelf is susceptible to hypoxia ($O_2 < 63$ mmol m^{-3}) in bottom waters

owing to the water-column stratification that develops after Mississippi River spring discharge (Wiseman et al. 1997). Following the onset of stratification, an expansive area of hypoxia is formed in the late spring and summer. The average hypoxic area from 1985 to 2007 was 13,500 km^2 (Rabalais et al. 2007).

Over the last several decades there has been active research exploring how riverine delivery of freshwater, nutrients, and organic matter relate to the extent and timing of hypoxia formation on the Louisiana shelf (reviewed by Rabalais et al. 2007; Dagg et al. 2007; Bianchi et al. 2010). By consensus, a primary mechanism for the development of hypoxia on this shelf is nutrient enhanced primary production that is subsequently respired in bottom waters. However, the myriads of water-column and sediment biogeochemical processes that interact to affect O_2 concentrations are complex and there are few measurements and large uncertainties for the magnitudes of carbon, O_2, and nutrient cycling processes across the Louisiana shelf; especially in the sediments (Dagg et al. 2007; Bianchi et al. 2010).

Though sediment-water fluxes of carbon, O_2, nitrogen, phosphorus, and silica have been described as potentially important sinks and sources on the Louisiana continental shelf (Eldridge and Morse 2008), measurements have been reported for only a few sites located on the eastern shelf, either beneath or adjacent to the Mississippi River plume (Gardner et al. 1993; Miller-Way et al. 1994; Morse and Rowe 1999; Rowe et al. 2002). There are no reported sediment-water flux rates from the western shelf (west of the Atchafalaya River outlet, >91.5°W), which annually has an expansive area of hypoxia that may equal or exceed the hypoxic area on the eastern shelf (Rabalais et al. 2002).

The role of sediments as a nitrogen sink on this shelf is largely unknown, but is likely to be significant through denitrification. Denitrification has been estimated to remove 30–60% of the annual nitrogen inputs to continental shelf systems (Seitzinger et al. 2006). This loss of fixed nitrogen is potentially an important moderator of primary production. Hypoxic conditions, though, have been observed to alter nitrogen fluxes by limiting coupled nitrification–denitrification and enhancing fluxes of NH_4^+ from the sediment (McCarthy et al. 2008; Middelburg and Levin 2009). Hence, under hypoxic conditions nitrogen may recycle many more times than under normoxic (100% O_2 saturation) conditions, and, thus, may support elevated rates of primary production across the shelf. For the Louisiana shelf, and marine systems in general, there are limited measurements and understanding of the strengths of such feedback mechanisms.

Spatial zones of similarity in sediment-water fluxes across the Louisiana shelf have been postulated due to differing degrees of freshwater influence, and, subsequently, variation in water-column primary production and organic matter deposition (Rowe and Chapman 2002; Dale et al. 2010). The zones of similarity for the Louisiana shelf have been described as a river plume region proximal to the discharge of the Mississippi and Atchafalaya Rivers (zone 1), an intermediate region adjacent to the plume with high rates of primary production (zone 2), a distant region with higher salinity and lower primary production (zone 3), and a region representing the inshore coastal current (zone 4). As in any dynamic system, zonal boundaries may not be fixed in time or space, but are useful for envisioning how the magnitudes of various biogeochemical processes influence the system. Identification of spatial patterns in sediment and water-column processes for the Louisiana shelf will improve the quantitative understanding of the processes that act as recyclers and sinks of nutrients and organic matter delivered by the Mississippi River watershed.

Materials and methods

The objectives of this study were to measure sediment-water fluxes of carbon, oxygen, nitrogen, phosphorus, and silica at sites distributed across the shelf, and to explore factors driving variability in sediment processes. Potential factors include riverine freshwater and nutrient loads, bottom-water O_2 concentrations, and water-column phytoplankton biomass and production. An emphasis of this study was to evaluate whether sediment-water fluxes were spatially coherent with the four zones of similarity (Rowe and Chapman 2002; Dale et al. 2010).

Study sites

During six cruises from 2005 to 2007, 23 stations were occupied in four study sites whose characteristics were consistent with those of the four zones of

similarity (Dale et al. 2010). Site Z01 (Fig. 1) was located adjacent to Southwest Pass, the largest of the passes from the lower Mississippi River to the Louisiana continental shelf, in a region that has been identified as the river plume (Green et al. 2006). Z02 was located to the west of the Mississippi River plume. Site Z03 was located on the western Louisiana shelf in a region of high salinity and low chl*a* concentration (Lehrter et al. 2009). Sites Z02 and Z03 both frequently experience hypoxia (Rabalais et al. 2002). Site Z04 was located in a region that is in the inshore region of the Louisiana coastal current (Wiseman et al. 1997). Z01, Z02, and Z03 had similar depths (19–22 m), whereas Z04 had shallower depths (5–8 m). During cruises when multiple stations were located within a site, average values of measurements (±standard error) were used.

River discharge and hydrographic data

Daily discharge data for the lower Mississippi and Atchafalaya Rivers were obtained from the US Army Corps of Engineers (gauge IDs 01100 and 03045, respectively) for the years 2005 to 2007. Estimated monthly nutrient loading data for the rivers were obtained for 2005–2007 from the US Geological Survey (Aulenbach et al. 2007). The discharge and nutrient data were used to evaluate the potential role of river forcing on sediment-water fluxes.

Sampling on the Louisiana continental shelf was performed from the OSV *Bold* for the five cruises during 2006 and 2007 and from the R/V *Longhorn* during the March 2005 cruise. At each site, vertical profiles of temperature, salinity, dissolved O_2, photosynthetically active radiation (PAR), and fluorescence were collected with a Sea-bird 911 CTD. Bottom-water samples for O_2 and nutrients were obtained from waters overlying sediment cores collected at the sites (see below for details on core collection).

Sediment-water fluxes

Sediment-water fluxes of DIC, O_2, N_2, and nutrients were measured in the dark with sediment chamber incubation methods modified from Cowan and Boynton (1996). During the five cruises in 2006 and 2007, sediment cores were collected with a hydraulically-dampened multi-corer (Ocean Instruments MC-400). The multi-corer was configured to collect four cores in Plexiglas chambers (10 cm ID × 40 cm). Following deployment and retrieval of the corer, sediments were inspected to ensure that the sediment surface layer was undisturbed. Generally, sediment cores passing inspection had visually apparent burrows and feeding tubes of benthic fauna at the sediment surface and clear overlying water. The in-situ water overlying the sediments was retained by the multi-corer (average depth of sediment from all cores was 18 cm). In March 2005, sediments were collected with a 0.25 m^2 box corer and sub-cored with the Plexiglas chambers. The chambers were gently pushed into the sediment surface, being careful not to disturb the surface sediment layer, and then excavated from the box corer. During retrieval of box cores, much of the bottom-water overlying the sediments drained from the surface of the core and, thus, was replenished with bottom-water carefully siphoned into the chambers until they were filled.

At each site, six sediment cores were collected in individual chambers; three were used for measurement of N_2 and O_2 fluxes and three were used for measurement of DIC and nutrient fluxes. Each triplicate set was submersed in a dark incubator filled with site bottom-water collected with a pump deployed from the ship. In addition to the triplicates, one chamber containing only bottom-water was incubated as a control. The incubator was maintained at ambient bottom temperatures (±0.5°C) using a thermostatically-controlled recirculating water bath. After submersion in the incubator, the sediment chambers were pre-incubated for at least 4 h while exposed to the large reservoir of site bottom-water in the incubator. This process allowed the sediments to equilibrate to the incubator conditions, while maintaining ambient bottom-water O_2 and nutrient concentrations overlying the cores through diffusional exchanges with the large volume (~0.5 m^3) of site bottom-water in the incubator.

Following the equilibration period, Plexiglas caps were fitted to seal the chambers. The caps were put in place while submerged in the incubator to avoid the introduction of gas bubbles. Once the caps were in place, the chambers remained closed until the end of the incubation. Within a chamber, the water overlying the sediment was mixed by a 2.5 cm magnetic stir bar suspended from the cap. The magnetic stir bars

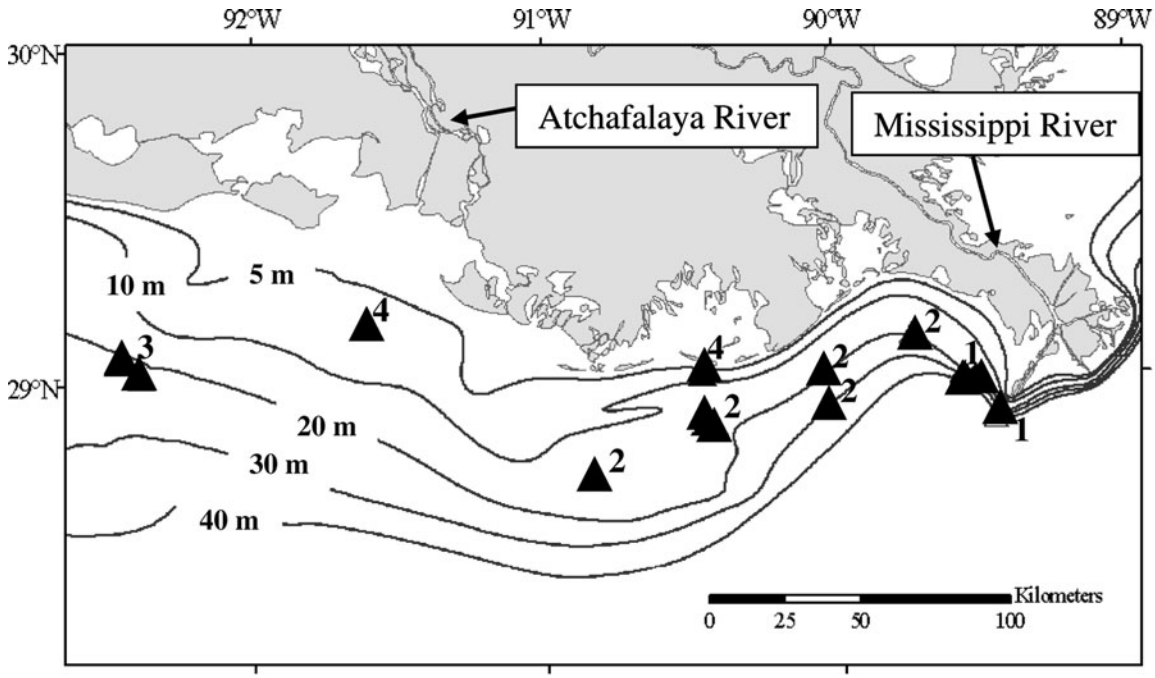
92°W
91°W
90°W
89°W
30°N
29°N
Atchafalaya River
Mississippi River
10 m
5 m
20 m
30 m
40 m
Kilometers
0 25 50 100

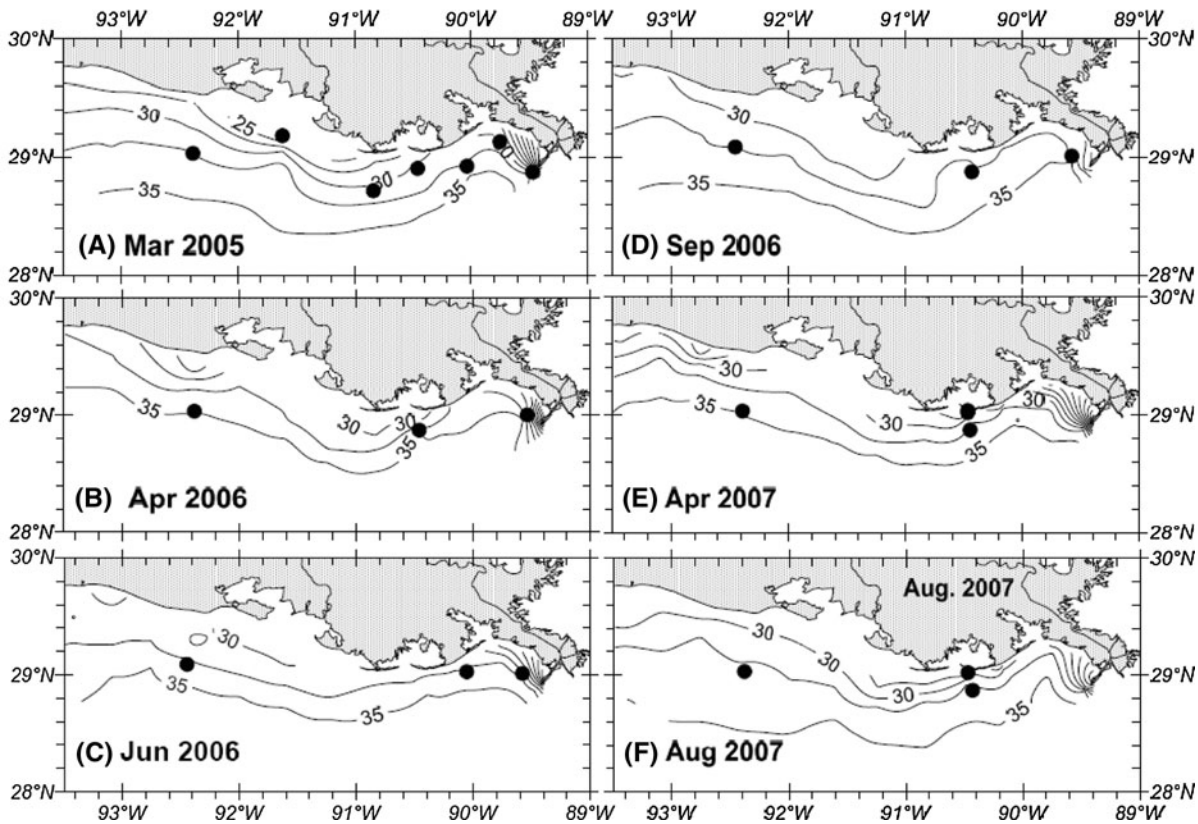
(A) Mar 2005
(B) Apr 2006
(C) Jun 2006
(D) Sep 2006
(E) Apr 2007
(F) Aug 2007
Aug. 2007
30°N
29°N
28°N
93°W
92°W
91°W
90°W
89°W

◀ **Fig. 1** Sediment sampling sites. (*Upper panel*) Black triangles represent the sites occupied during six spring and summer cruises from 2005 to 2007. *Bold numbers* (1–4) represent how the sites were aggregated according to proposed zones of similarity (Rowe and Chapman 2002; Dale et al. 2010). *Black lines* with labels are bathymetry contours (m). (*Lower panels*) Sediment stations occupied on each cruise (*black circles*) overlaid on surface salinity contours (*black lines*) mapped from shelf-wide surveys that occurred directly before or after sediment sampling

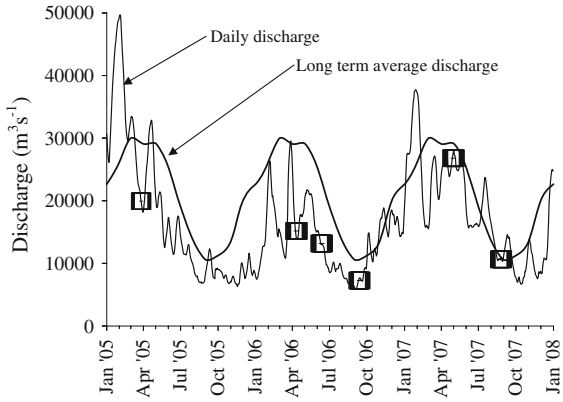

Fig. 2 Total Mississippi and Atchafalaya River discharge to the Louisiana continental shelf. *Thick black line* indicates long term average discharge. *Black framed windows* represent the cruise dates during which sediment-water fluxes were measured. Discharge data obtained from the U.S. Army Corps of Engineers for the lower Mississippi River (Gage ID 01100) and the lower Atchafalaya River (Gage ID 03045)

for the three sediment chambers and the one control (i.e. bottom-water only) chamber were stirred (~45 RPM) simultaneously by an external motor that turned a circular plate mounted with four magnets.

Sampling of the chambers without removing the caps was facilitated by inlet and outlet ports plumbed through the core cap. The inlet port was gravity-fed through tubing from a 5-l carboy filled with site bottom-water. Collecting an overlying water sample from the chamber entailed opening the inlet port to allow a volume of bottom-water into the chamber and thereby displace an equal volume through the outlet port. Keeping the chambers sealed throughout the incubation reduced the potential for contamination by atmospheric gases, especially N_2, and solutes that may have otherwise occurred with invasive sampling. Samples were collected approximately every 2 h (four to seven samples) during 8–16 h incubations.

Dissolved N_2, O_2, and Ar samples were collected in duplicate in 7-ml glass test tubes. Samples were fixed with 20 μl of 5% $HgCl_2$, tightly sealed with ground glass stoppers, and stored submerged in chilled seawater for 1–2 weeks until analyzed. Laboratory tests indicated the glass-stoppered test tubes maintained constant N_2, O_2, and Ar concentrations for several weeks to a month (data not shown). Dissolved gas analyses were conducted on a Pfeiffer Prisma quadrupole mass spectrometer fitted with a membrane inlet (Kana et al. 1994).

DIC analyses were conducted shipboard, immediately after collection, on unfiltered samples with a Shimadzu TOC-5000 carbon analyzer calibrated with a certified seawater DIC standard (Scripps Institute of Oceanography). Ammonium (NH_4^+) analyses were performed shipboard on filtered (GF/F) samples using the fluorometric method described by Holmes et al. (1999). Samples for nitrate + nitrite (NO_3^-), dissolved inorganic phosphorus (DIP), and silicate (SiO_2) were filtered through GF/F filters and stored at −70 °C until analysis. NO_3^-, NO_2^-, DIP, and SiO_2 concentrations were measured (APHA 1989) on a continuous flow auto-analyzer (Astoria-Pacific).

The sediment-water flux (mmol m^{-2} day^{-1}) of a constituent was calculated as

$$\text{sediment-water flux} = (m_{\text{sediment}} - m_{\text{bottom-water}}) \times z_{\text{overlying water}} \quad (1)$$

where m_{sediment} was the rate of change in concentration for waters overlying sediment cores obtained from linear regression of the sample concentrations versus time, $m_{\text{bottom-water}}$was the rate of change in concentration for the bottom-water control, and $z_{\text{overlying water}}$ was the water depth (m) in the Plexiglas chamber. Overlying water concentrations were not corrected for refill water concentrations as the volume of refill water was never more than 2% of the total overlying water volume, and, therefore, was assumed to be a small contribution to the overall concentration trend versus time. Confidence intervals were used to evaluate whether a slope was significantly different from zero ($\alpha = 0.20$). Slopes not significantly different from zero were set equal to zero. Generally, a slope not significantly different from zero resulted from small changes in concentration during the incubation. Positive fluxes indicated a net efflux out of the sediments.

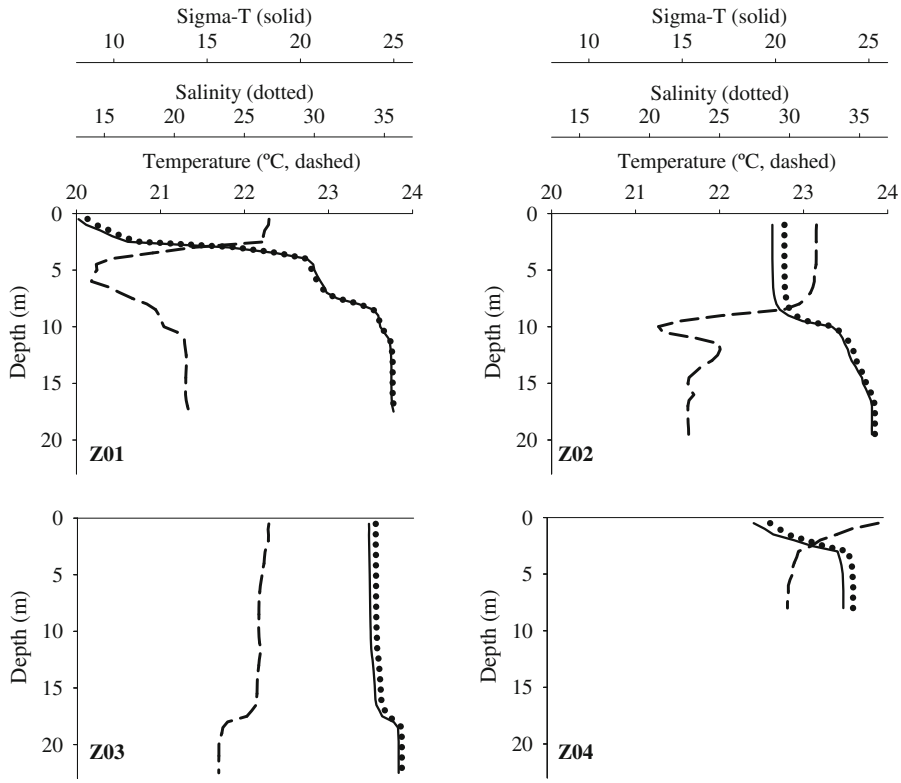

Fig. 3 Representative hydrographic profiles of temperature, salinity, and density (Sigma-T). The Z01, Z02, and Z03 profiles were observed April 2006. The Z04 profile was observed April 2007

Sediment bulk analyses

Sediment porosity, organic carbon, organic nitrogen, organic phosphorus, and chl*a* were measured on surficial sediments (top 1–2 cm) that were frozen (−20°C) until laboratory analysis. From the box corer, surface sediment samples were collected from unused portions of the box core. From the multicorer, surface sediment samples were obtained from another set of cores collected at the same time as cores used for flux measurements. Porosity was calculated as dry bulk density divided by the particle density where particle density was taken to be 2.6 g cm^{-3}. For chemical analyses of the sediments, sediments were dried, milled to a powder, and fumed with HCl to volatilize inorganic carbon. Sediment organic carbon and nitrogen concentrations were measured following high temperature combustion on an Elementar Vario EL elemental analyzer. Sediment organic phosphorus concentrations were calculated as the difference of sediment total phosphorus and sediment inorganic phosphorus determined following the method of Aspila et al. (1976). Chl*a* concentrations were determined fluorometerically on extracts obtained with 0.5 g sediment in 10 ml of 90% buffered methanol (Welschmeyer 1994).

Phytoplankton biomass and production rates

Water-column samples of chl*a* were collected at multiple depths, surface and bottom at a minimum, and analyzed fluorometrically (Welschmeyer 1994). Phytoplankton photosynthesis-irradiance (PE) experiments were conducted at each station. During March 2005 one PE experiment per station was performed. On the 2006 and 2007 cruises, the sites were occupied for over a diel cycle, thus allowing multiple (3–7) PE experiments to be performed at each site. The PE methods and models used to estimate primary production rates have been presented in detail elsewhere (Lehrter et al. 2009). Phytoplankton biomass and production rates were compared to sediment-water fluxes to identify the degree of potential coupling between primary production and sediment-water fluxes of carbon, oxygen, and nutrients.

Table 1 Averages and standard errors (SE) of site bottom water and particulate sediment concentrations

Site	O_2	SE	NO_3^-	SE	NH_4^+	SE	DIP	SE
Bottom water								
Z01	104.3	21.3	6.91	2.58	1.14	0.57	0.61	0.15
Z02	58.7	20.6	7.04	1.11	2.39	1.01	1.19	0.31
Z03	109.8	23.9	2.15	0.76	1.61	0.57	0.66	0.22
Z04	125.5	10.2	5.47	4.52	4.85	0.77	0.54	0.08
Site	OC	SE	ON	SE	OP	SE	Sed Chl*a*	SE
Sediment								
Z01	0.38	0.27	0.034	0.027	0.0028	1.79E−06	1.11	0.31
Z02	1.06	0.11	0.091	0.010	0.0032	6.03E−07	1.55	0.27
Z03	0.66	0.06	0.061	0.006	0.0034	2.54E−07	1.03	0.19
Z04	0.31	0.01	0.021	0.001	0.0012	7.15E−07	1.56	0.44

Bottom water concentrations (mmol m^{-3}) measured were dissolved oxygen (O_2), nitrate + nitrite (NO_3^-), ammonium (NH_4^+), and dissolved inorganic phosphorus (DIP). Particulate sediment concentrations (mmol gdw^{-1}) measured were organic carbon (OC), organic nitrogen (ON), organic phosphorus (OP), and sediment chl*a* (μg gww^{-1})

Statistical analyses

Analysis of variance (ANOVA) was used to assess differences across sites and across cruises. Least squares regresssions were used to estimate sediment-water flux rates and to evaluate relationships between potential forcing factors and flux rates.

Results

Mississippi river discharge and shelf hydrographic conditions

Sampling occurred over variable Mississippi and Atchafalaya River discharge regimes (Fig. 2). The March 2005, April and June 2006, and August 2007 cruises occurred on the falling limbs of peaks in the discharge hydrograph. A period of sustained low discharge preceded the September 2006 cruise (July–September mean discharge = 7,993 m^3 s^{-1}), while a period of sustained high discharge preceded the April 2007 cruise (February–April mean discharge = 23,967 m^3 s^{-1}).

Vertical profiles of water-column temperature, salinity, and density (Fig. 3) varied among the sites, though bottom-water salinity was similar (>35). Z01 had the lowest surface salinities (average = 22.7) and shallowest pycnoclines (average = 6.8 m). Z02 generally had a well-mixed surface layer (average surface salinity = 29.7) and a strong pycnocline at a depth of approximately 10 m. In the late summer, however, the vertical profiles at Z02 were more similar to those observed at Z03, which generally had higher salinity in the surface layer (average surface salinity = 32.2) and an average pycnocline depth of 13 m. Z04, located in the coastal current, had an average surface salinity of 28.9, and had a shallow pycnocline at about 2.1 m depth. Bottom-water temperatures across all sites ranged from 20.0°C in the spring to 30.0°C in the summer.

Water-column O_2 concentration profiles (data not shown) were generally uniform in the surface-mixed layer and decreased below the pycnocline. Hypoxic conditions in the bottom waters were encountered in April 2006 at Z01 and Z02, June 2006 at Z02, September 2006 at Z02, and August 2007 at Z02 and Z03. The lowest O_2 concentrations (12–16 mmol m^{-3}) were encountered in August 2007. Over the course of the study, average bottom-water O_2 concentrations at the sites were ordered from minimum to maximum as Z02 < Z03 < Z01 < Z04 (Table 1).

Average nutrient concentrations in the bottom waters (Table 1), were typically highest at Z02 where the NO_3^- and DIP concentrations were 7.0 and 1.2 mmol m^{-3}, respectively. Bottom-water NO_3^- concentrations at Z01 (average = 6.9 mmol m^{-3}) and Z04 (average = 5.5 mmol m^{-3}) were also similar

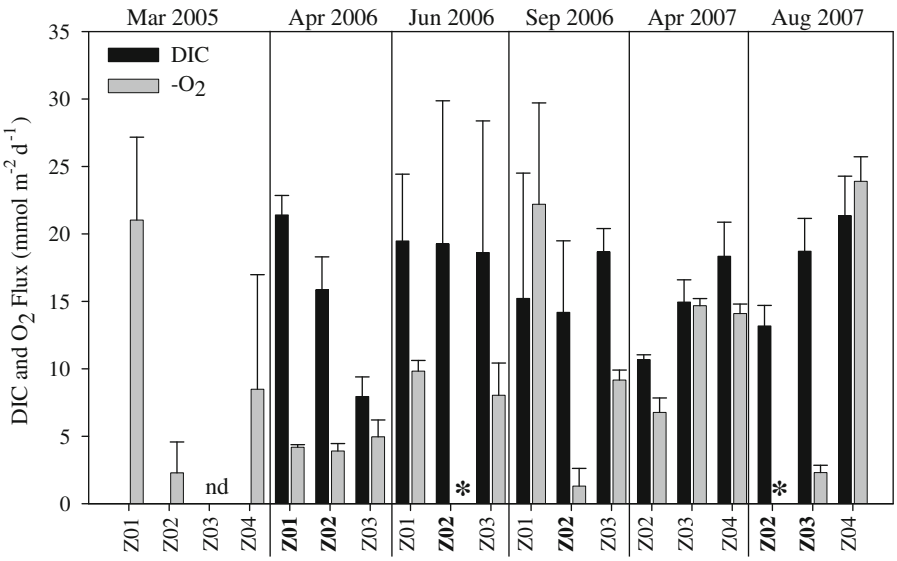

Fig. 4 Dissolved inorganic carbon (DIC) and oxygen (O_2) fluxes at the sites occupied on each cruise. O_2 fluxes, which were negative by convention in this study, are displayed as positive values for comparative purposes. *Error bars* represent the standard error. *Bold site* names indicate the overlying water in the sediment chambers was hypoxic. DIC fluxes were not measured in March 2005. O_2 fluxes were not measured at site Z03 in March 2005 (*nd* no data). *O_2 fluxes were zero at site Z02 during June 2006 and August 2007

Table 2 Sediment-water flux averages (mmol m^{-2} day^{-1}) and standard errors (SE) by cruise and site of nitrate + nitrite (NO_3^-), ammonium (NH_4^+), inorganic phosphorus (DIP), inorganic silica (Si) and nitrogen gas (N_2)

Date	Site	NO_3^-	SE	NH_4^+	SE	DIP	SE	Si	SE	N_2	SE
Mar 2005	Z01									0.16	0.16
	Z02	−0.23	0.15	0.59	0.40	−0.19	0.18	1.55	1.01	1.04	0.47
	Z03	0.32	0.32	0.67	0.19	0.11	0.11	4.44	0.69		
	Z04	1.03	0.19	−0.07	0.07	−0.09	0.09	0.66	0.66	3.03	0.20
Apr 2006	Z01	−0.20	0.10	0.34	0.13	0.04	0.01	2.13	0.32	0.00	0.00
	Z02	0.01	0.08	0.37	0.03	0.02	0.01	2.49	1.26	0.18	0.07
	Z03	0.15	0.02	0.04	0.01	0.01	0.02	0.23	0.01	0.17	0.02
Jun 2006	Z01	0.33	0.03	0.25	0.11	0.04	0.02	2.15	0.24	1.34	0.10
	Z02	−1.01	0.07	3.84	0.61	0.05	0.04	2.51	0.33	0.20	0.20
	Z03	0.20	0.06	0.37	0.32	−0.04	0.04	2.28	0.60	0.88	0.31
Sep 2006	Z01	0.44	0.14	0.05	0.02	0.06	0.03	2.17	0.20	0.27	0.07
	Z02	−0.32	0.04	0.37	0.03	0.14	0.03	1.93	0.35	0.40	0.16
	Z03	−0.08	0.00	0.48	0.08	0.00	0.00	1.57	0.12	0.25	0.03
Apr 2007	Z02	0.12	0.02	0.38	0.18	0.05	0.00	1.64	0.18	0.94	0.12
	Z03	0.03	0.03	−0.14	0.07	0.01	0.00	0.34	0.06	0.19	0.13
	Z04	0.08	0.02	0.91	0.15	0.03	0.01	1.16	0.13	0.00	0.00
Sep 2007	Z02	−0.36	0.02	0.67	0.09	0.26	0.08	2.08	0.26	0.49	0.13
	Z03	−0.17	0.00	−0.17	0.25	−0.11	0.08	0.26	0.26	1.80	0.25
	Z04	−0.04	0.01	1.02	0.29	0.05	0.05	1.55	0.36	1.23	0.71

Some fluxes were not measured in March 2005

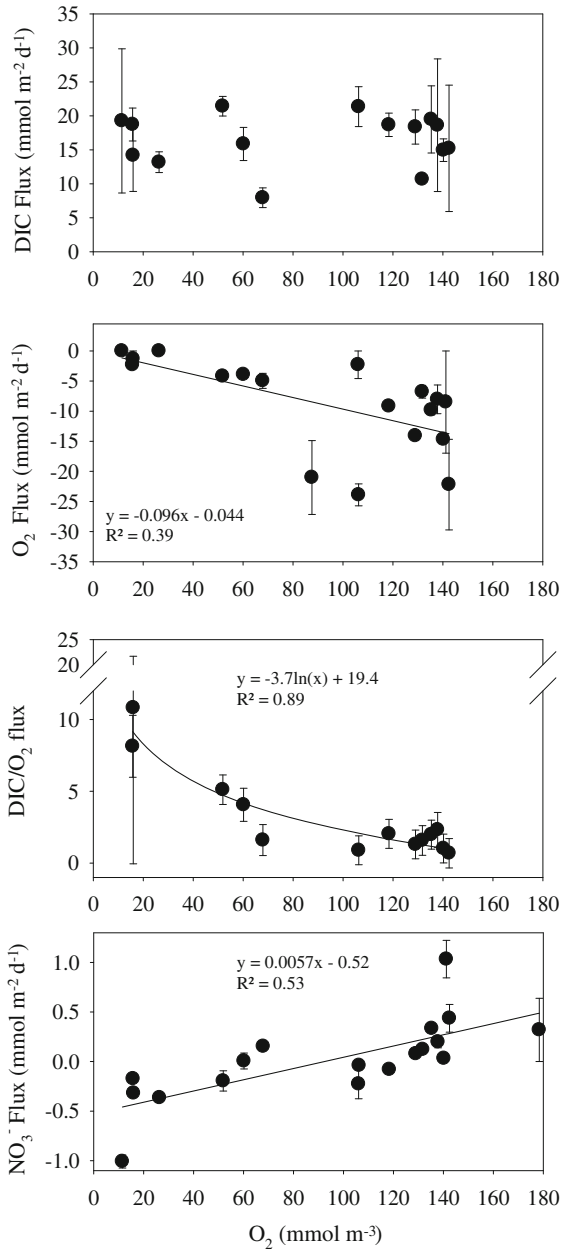

Fig. 5 Bottom water O_2 concentration relationships with sediment DIC flux, O_2 flux, the DIC/O_2 flux ratio, and NO_3^- flux. Regression relationships of O_2 concentration with O_2 flux and NO_3^- flux were linear fits. The regression relationship of O_2 concentration with the DIC/O2 flux ratio was a lognormal fit

to those observed at Z02. Z03 typically had the lowest bottom-water NO_3^- (average = 2.2 mmol m^{-3}). Highest bottom-water NH_4^+ levels were observed at Z04 (average = 4.9 mmol m^{-3}).

Sediment characteristics

Porosity in the surface sediments were similar at Z01 and Z04 with averages (±SE) being 0.6 (±0.1) and 0.5 (±0.01), respectively (data not shown). Z02 and Z03 had higher average porosity of 0.8 (±0.04) and 0.8 (±0.03), respectively. Sediment carbon, nitrogen, and phosphorus concentrations (Table 1) were largest at Z02 and Z03, whereas chl*a* concentrations (Table 1) at the sites were not statistically different due to high variability across cruises.

Sediment-water fluxes

There were no significant differences in fluxes by cruise (ANOVA) despite high variability in river discharge preceding each cruise. Also, site-specific regression analyses between sediment-water fluxes, river discharge, and NO_3^- loads did not yield significant relationships. The lack of significance may be partially attributed to low degrees of freedom (df = 2–5) for the regression statistics.

DIC fluxes ranged from 7.9 to 21.4 mmol m^{-2} day^{-1} (Fig. 4), but did not exhibit differences by site (ANOVA, $P = 0.65$) owing to high variability. Site average DIC fluxes ± standard error were 18.7 ± 1.8, 14.6 ± 1.4, 15.8 ± 2.1, and 19.8 ± 1.5 at Z01, Z02, Z03, and Z04, respectively. O_2 fluxes ranged from 0 to −23.9 mmol m^{-2} day^{-1} (Fig. 4), and were

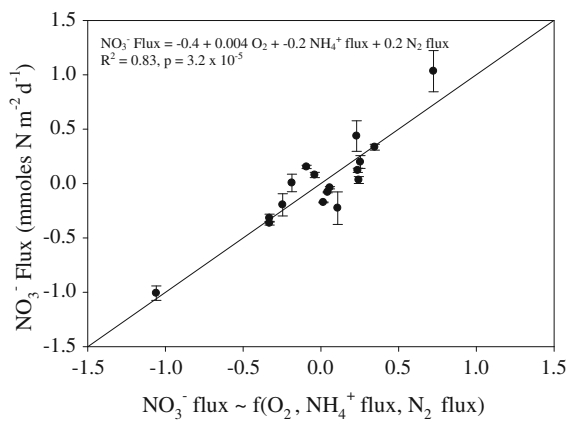

Fig. 6 NO_3^- flux multiple regression relationship with bottom-water O_2 concentration, NH_4^+ flux, and N_2 flux. The regression equation contains the intercept and the coefficients for O_2, NH_4^+ flux, and N_2 flux. The coefficient of determination (R^2) and P-value for the regression model are shown. *Error bars* are the standard error for each NO_3^- flux measurement

significantly different among sites (ANOVA, $P = 0.04$). Largest O_2 fluxes into the sediments occurred at Z01 and Z04 (average = −14.3 and −15.5 mmol m^{-2}−day^{-1}, respectively) and lowest O_2 fluxes occurred at Z02 and Z03 (average = −2.4 and −7.8 mmol m^{-2}−day^{-1}, respectively).

Sediment NO_3^- fluxes ranged from −1.01 to 1.03 mmol m^{-2} day^{-1} (Table 2) and varied by site (ANOVA, $P = 0.09$). Z01 and Z04 sediments were, on average, net sources of NO_3^- with average fluxes of 0.19 and 0.36 mmol m^{-2} day^{-1}, respectively. During 4 of the 6 cruises Z02 was a net sink of NO_3^- and had an overall average flux of −0.30 mmol m^{-2} day^{-1}. Sediment NH_4^+ fluxes ranged from −0.17 to3.84 mmol m^{-2} day^{-1} (Table 2), but did not vary by site (ANOVA, $P = 0.46$). Most of the NH_4^+ fluxes were directed out of the sediments, but small fluxes of NH_4^+ into the sediment (−0.07 to −0.17 mmol m^{-2} day^{-1}) were observed at Z04 during March 2005 and Z03 during April 2006 and April 2007.

Sediment DIP fluxes ranged from −0.19 to 0.26 mmol m^{-2}−day^{-1} (Table 2), but did not vary by site (ANOVA, $P = 0.71$). DIP effluxes from the sediment were most common (14 of 18 observations). Sediment Si fluxes ranged from 0.23 to 4.44 mmol m^{-2} day^{-1} (Table 2), but were not statistically different across sites (ANOVA, $P = 0.53$).

Sediment N_2 fluxes ranged from 0 to 3.03 mmol m^{-2} day^{-1} (Table 2). N_2 fluxes were highly variable, but most of the observations (11 of 18) fell within a small range (0 to 0.49 mmol m^{-2} day^{-1}). Observations of N_2 fluxes greater than 1 mmol m^{-2} day^{-1} occurred for 5 of 18 observations. As a result of the high variability, average N_2 fluxes did not vary significantly by site (ANOVA, $P = 0.38$). The N_2 flux average for the study was 0.70 mmol m^{-2} day^{-1} (SE = 0.04, $n = 18$).

Relationships among sediment-water fluxes and other variables

Under normoxic conditions, DIC and O_2 fluxes were not significantly different from one another (Fig. 4). However, under hypoxic conditions DIC fluxes were much larger than O_2 fluxes. DIC fluxes did not covary with bottom-water O_2 concentrations ($P = 0.9$), and the magnitude of DIC fluxes during hypoxic events (average = 16.3 mmol m^{-2} day^{-1}) did not differ from DIC fluxes measured under normoxic conditions (average = 16.6 mmol C m^{-2} day^{-1}). In contrast, sediment O_2 flux rates strongly covaried with bottom-water O_2 concentrations ($r = -0.62$, $P = 0.006$, $n = 18$) with rates approaching zero when overlying O_2 concentrations were depleted (Fig. 5). This was the case most often at site Z02 which typically had the lowest bottom-water O_2 concentrations (average = 59 mmol m^{-3}) and the smallest O_2 fluxes (average = −2.4 mmol m^{-2} day^{-1}). Z01 and Z04 had the highest bottom-water O_2 concentrations (Table 1) and the highest O_2 fluxes (Fig. 4). The DIC/O_2 flux ratio, an indicator of the sediment re-oxidation efficiency, also varied as a function of O_2 concentration (Fig. 5).

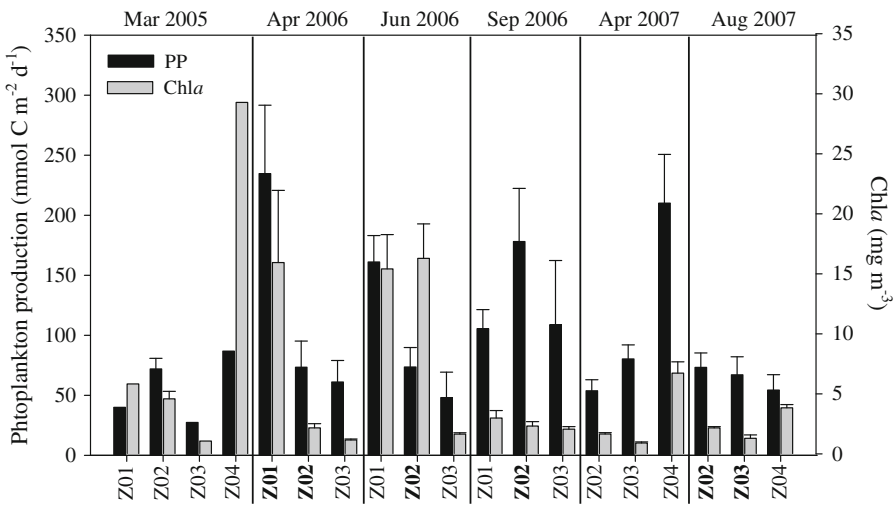

Fig. 7 Average phytoplankton production (*left axis*, PP) and chl*a* in the euphotic zone (*right axis*). *Error bars* represent the standard error. *Bold site* names indicate the bottom waters were hypoxic. Replicate measures of primary production and chl*a* were not made for most sites in March 2005

Table 3 Averages (percents) and ranges (in parentheses) of potential contributions of sediment nutrient fluxes to nutrient demand by primary production (PP) in the entire water column and in the sub-pycnocline water column

Site	Contribution to total water column PP			Contribution to sub-pycnocline PP		
	DIN	DIP	Si	DIN	DIP	Si
Z01	2 (0–3)	4 (2–6)	10 (6–14)	66 (13–121)	108 (59–136)	309 (194–448)
Z02	7 (0–26)	11 (0–37)	18 (7–23)	48 (0–123)	36 (0–84)	155 (13–368)
Z03	6 (0–16)	7 (0–41)	26 (2–108)	43 (0–228)	95 (0–581)	277 (4–1509)
Z04	7 (3–12)	4 (0–9)	9 (4–19)	60 (4–161)	5 (0–13)	47 (5–110)

N, P, and Si phytoplankton demand were calculated based on primary production rates measured in units of carbon and converted to equivalent nutrient demand rates using Redfield stoichiometry

NO_3^- fluxes were positively correlated with bottom-water O_2 concentrations (Fig. 5). NO_3^- fluxes were also significantly correlated with NH_4^+ fluxes ($r = -0.69$, $P = 0.001$, $n = 18$) and N_2 fluxes ($r = 0.54$, $P = 0.02$, $n = 17$). A significant correlation between NO_3^- flux and bottom-water NO_3^- concentration was not observed ($P = 0.90$). A multiple linear regression model, NO_3^- flux ~ f(O_2, NH_4^+ flux, N_2 flux), explained a large fraction of the variability in NO_3^- flux ($R^2 = 0.83$, Fig. 6). N_2 fluxes were not directly correlated with bottom-water O_2 concentrations, sediment O_2 fluxes, or bottom-water NO_3^- concentrations ($P = 0.39$, 0.76, and 0.50, respectively).

Site water-column chl*a* measurements (described below) were correlated with both DIC ($r = 0.55$, $P = 0.04$, $n = 15$) and N_2 ($r = 0.50$, $P = 0.04$, $n = 15$) fluxes. DIP fluxes were significantly correlated to sediment surface chl*a* concentration ($r = 0.61$, $P = 0.02$, $n = 15$). None of the fluxes were significantly correlated with temperature.

Water-column phytoplankton biomass and primary production

Chl*a* concentrations averaged over the euphotic depth (i.e., the depth of 1% surface light) were 10.0, 4.9, 1.4, and 13.3 mg m^{-3} at Z01, Z02, Z03, and Z04, respectively. Z03 and Z04 had chl*a* concentrations significantly higher than Z02 and Z03 (ANOVA, $P = 0.05$). Phytoplankton primary production rates (Fig. 7) ranged from 27 to 235 mmol C m^{-2} day^{-1}. Primary production rates at Z01 in April and June 2006 (235 and 161 mmol Cm^{-2} day^{-1}, respectively) were significantly greater than at Z02 and Z03. The lowest salinities (18.0 and 22.6, respectively) were observed at Z01 during these dates. Rates of primary production at Z04 (210 mmol C m^{-2} day^{-1}) were significantly greater than at Z02 and Z03 during April 2007, and corresponded with the lowest salinity (29.4) observed on that cruise. Z02 and Z03 had statistically similar primary production rates on all 5 cruises.

As a result of low light attenuation and shallow pycnocline depths, significant fractions of water-column primary production occurred beneath the pycnocline. At Z02, Z03, and Z04 the percentage of primary production occurring beneath the pycnocline averaged 26, 30, and 50%, respectively. In contrast, at Z01 where light attenuation was highest, only 7% of the primary production, on average, occurred beneath the pycnocline. The percentage of primary production below the pycnocline is likely to be a conservative estimate for Z02 and Z03 which were located in regions of the shelf with low light attenuation, hence large amounts of light reaching the bottom (Lehrter et al. 2009), and, thus, potential for benthic primary production (Dortch et al. 1994).

Sediment-water fluxes in comparison to water-column primary production

On average, the fraction of carbon fixation by water-column primary production accounted for by the sediment DIC fluxes was 12, 19, 23, and 24% at stations Z01, Z02, Z03, and Z04, respectively. Site average sediment DIN and DIP fluxes, when positive, could potentially supply 2–7 and 4–11%, respectively, of the water-column integrated primary production nutrient demand calculated according to the Redfield ratio (Table 3). Assuming the water-column phytoplankton were dominated by diatoms (J. Kurtz

unpublished data) and that diatoms require Si in the same ratio as nitrogen (i.e. Redfield), sediment Si fluxes could supply 9–26% of the phytoplankton demand. For the sub-pycnocline portion of the water-column, sediment nutrient fluxes potentially provided a large fraction of the nutrients required by phytoplankton (Table 3). On average, DIN fluxes could provide 43–66% and DIP fluxes could provide 5–108% of the sub-pyncocline phytoplankton demand. The observations of nutrient fluxes directed into the sediments (Table 2) indicated that at times the sediment community exerted a nutrient demand equal to or greater than the water-column demand.

Discussion

Prior to this study, published DIC and nutrient flux rates were limited to cruises from July 1990, April 1992, and August 1994 (Gardner et al. 1993; Miller-Way et al. 1994; Rowe et al. 2002). These studies were all conducted at sites in the vicinity of the Mississippi River plume on the eastern shelf. The only published estimates of denitrification rates were from the July 1990 cruise, which were estimated indirectly by stoichiometry from nutrient and O_2 flux rates (Gardner et al. 1993). Sediment O_2 flux measures were recently reported for 10 cruises from 2003 to 2007 (Murrell and Lehrter 2011). The O_2 fluxes reported herein from 2005 to 2007 were measured at the same locations as in Murrell and Lehrter (2011). However, the O_2 flux data presented in this study are independent observations as the measurements were made on separate sets of triplicate cores using different methods.

Methodological considerations for sediment-water fluxes

Sediment-water flux rates determined from in situ chamber measurements and shipboard chamber measurements have been shown to be equivalent (Miller-Way et al. 1994). Sediment-water flux measurements in chambers, however, are susceptible to methodological artifacts that may affect observations. These artifacts arise from the sensitivity of fluxes to bottom-water O_2 concentrations, hydrodynamics, and the activity of benthic fauna. Bottom-water O_2 concentrations strongly regulate the depth of O_2 penetration depth in the sediments and, thus, the sediment-water O_2 flux rates (Cai and Sayles 1996). Bottom-water O_2 also affects the fluxes of NH_4^+, NO_3^-, and N_2 by altering nitrification–denitrification rates (McCarthy et al. 2008; Middelburg and Levin 2009) and the fluxes of DIP through iron sorption and desorption of phosphate under oxic and anoxic conditions, respectively (Roden and Edmonds 1997). Altered hydrodynamics within chambers may serve to increase or decrease the transport of solutes into the sediments and, thus, affect their exchange rates (Glud 2008). Finally, chambers may under-represent benthic fauna that actively irrigate and enhance diffusion into the sediments through their burrows and that stimulate microbial activity through their metabolic activities (e.g. Aller and Aller 1986; Pelegri et al. 1994). Researchers using chambers should evaluate how these potential artifacts affect their measured rates.

In the present study, 12–16 h incubations were employed to determine sediment-water fluxes. As a consequence of these incubation times, on average there was a 36% decrease in O_2 concentration over the incubation period. It has been suggested that O_2 changes of greater than 10–15% from initial conditions will induce a non-linear change in O_2 flux rates (Glud 2008), which may affect other flux rates based on their dependence on O_2. In the present study, however, the linear approximation used to calculate the rate of change in the chamber incubations (i.e. $m_{sediment}$, Eq. 1) appeared to be a robust estimate as average R^2 from the linear regressions ranged from 0.7 to 0.9. It is recommended that for cases, such as encountered here, where the O_2 concentration is expected to drop significantly that time points be collected every 1–2 h to evaluate linearity.

Chamber alterations to hydrodynamics are also known to affect flux rate measurements. Isolating the sediments with a chamber changes the water flow over the sediment surface. In permeable, sandy sediments, advective transport of solutes into sediment porewaters may be significant (Huettel and Webster 2001). However, in the impermeable, muddy sediments of the Louisiana shelf, 75% silt + clay on average (Murrell and Lehrter 2011), exchanges between bottom-water and sediment porewaters will be controlled by diffusive processes. Chamber effects on diffusion across the sediment-water interface primarily occur through changing the thickness of the diffusive boundary layer. The consensus

from numerous studies of various chamber designs (reviewed by Glud 2008) is that this effect is likely to be small for sediments with an O_2 penetration depth greater than a couple of mm. For the sites visited in this study, the average O_2 penetration depth, calculated from Cai and Sayles (1996, Eq. 7A), was 2.3 mm (range = 0.3–5.5 mm). For perspective on how much a change in the thickness of the diffusive boundary layer might affect the average rates reported herein, a modeling study of sediments, which had a range of O_2 penetration depths from 0.6 to 4.6 mm, indicated that the reduction in thickness of the diffusive boundary layer from 900 to 0 μm enhanced the calculated annual O_2 consumption rate by 10% (Glud et al. 2007).

Another consideration for chamber effects on hydrodynamics is that it is necessary to stir the waters overlying the sediments in order to eliminate concentration gradients. Stirring is typically done with a magnetic stir bar driven by an external motor turning a magnet, and may enhance solute exchange with the sediments by advective or diffusive, i.e. reducing or eliminating the diffusive boundary layer, processes. To our knowledge, there have not been any studies that have quantified the impact of stirring rates on sediment-water fluxes for muddy sediments. In a study of sediment-water exchanges in sandy sediments it was observed that O_2 and DIC fluxes were similar for stirring rates < 50 RPM, but flux rates increased at higher stirring rates (Cook et al. 2007). The chambers in the present study were stirred at a rate of 45 RPM which was observed to maintain a mixed water-column in the chamber, and, based on the work by Cook et al. (2007), likely did not significantly alter sediment-water flux rates.

Bias in measured exchange rates may also occur if the benthic fauna are disturbed or undersampled. Benthic fauna affect sediment-water exchanges through irrigation and enancement of diffusion (Aller and Aller 1986) and are known to enhance denitrification rates (Pelegri et al. 1994). The direct impact of the fauna on fluxes was not evaluated in this study. However, burrows and organisms inhabiting them were visually identified in many of the chambers and the largest within site variability in sediment-water exchange rates (standard errors in Fig. 4; Table 2) occurred at sites where a sediment chamber captured one or more large burrow-dwelling organisms. Inclusion of benthic fauna in a sample is controlled by both the size of the chamber and the number of replicates. A simulation study of the effects of chamber size on calculated O_2 flux rates, indicated that chambers with a radius of 5 cm had O_2 exchange rate inaccuracies >25% (Glud and Blackburn 2002). Increasing the chamber size and the number of replicates reduced inaccuracies. Chambers with a radius of 10 cm and $n = 3$ (the radius and number of replicates used herein) had simulated inaccuracies of ~7 to 18%.

A known bias of flux estimates is the area of the sediment surface in the chamber. The sediment surface has topographic relief and has been observed to be 7–12% larger than the planar surface, resulting in a 1.14 to 1.25-fold adjustment to rates calculated assuming a flat surface (Røy et al. 2005). Further work is needed to assess how these potential artifacts and bias interact to alter chamber-based flux rate estimates in comparison to in situ rates.

Characterization of sediment-water fluxes on the Louisiana shelf

Although the cruises occurred over a wide range of river discharge, there were no significant relationships between fluxes and either river discharge, nutrient load, or nutrient concentrations. It is likely that river discharge and loads influenced sediment respiration to some degree, but the small number of observations may not have been sufficient to demonstrate this relationship. It is also likely that seasonal sediment transport events occurring with tropical storms (Goñi et al. 2006; Sampere et al. 2008) and winter cold fronts (Walker and Hammack 2000) serve to homogenize the sediments at the annual scale and thus obscure smaller temporal variations that would occur in response to seasonal river nutrient and organic matter fluxes.

DIC and O_2 fluxes

In the dark, sediment DIC fluxes approximate net CO_2 production and as such are a proxy for sediment respiration (Hopkinson and Smith 2005). DIC fluxes were generally greater than absolute values of O_2 fluxes (Fig. 4) and DIC flux rates were insensitive to changes in overlying bottom-water O_2 concentration (Fig. 5). The DIC/O_2 flux ratio was was observed to increase as O_2 concentrations were depleted (Fig. 5).

This ratio reflects the efficiency of reoxidation of NH_4^+ and reduced iron, manganese, and sulfur. Hence, sites with high DIC/O_2 flux ratios were accumulating a chemical oxygen debt because there was not enough O_2 in the overlying water to efficiently reoxidize the reduced products of anaerobic metabolism. These results are consistent with anaerobic respiration being the dominant organic carbon mineralization pathway in coastal sediments and a large portion of the O_2 flux into the sediment resulting from reoxidation of reduced species created as end products of anaerobic respiration (Jørgensen 1982; Sampou and Oviatt 1991; Aller et al. 1996). For example, nitrification, calculated as the sum of N_2 and NO_3^- fluxes (Fennel et al. 2009), potentially accounted for 24% of the sediment O_2 demand in this study. A meta-analysis of nitrification in aquatic sediments determined a similar estimate of 17% (Fennel et al. 2009).

A previous study reported DIC fluxes averaging (±SE) 31.1 (±8.7) mmol m^{-2} day^{-1} at sites near Z01 and Z02 (Rowe et al. 2002). However, the fluxes measured by Rowe et al. (2002) were not corrected for changes that could be attributed to the bottom-water alone. For the data reported herein, if we neglect the DIC fluxes observed in the bottom-water controls, the average sediment + bottom DIC flux would be 23.9 (±1.9) mmol m^{-2} day^{-1}, which is lower, but not significantly different than Rowe et al.'s (2002) average. Site average DIC fluxes measured in this study were not statistically different from one another (Fig. 4), but had a pattern where the highest average fluxes (19.8 and 18.7 mmol C m^{-2} day^{-1}) occurred in the coastal current (Z04) and plume (Z01) regions and lower DIC fluxes (14.6 and 15.8 mmol m^{-2} day^{-1}) occurred at sites Z02 and Z03. Average DIC fluxes across all cruises (16.6 mmol m^{-2} day^{-1}) were similar to DIC fluxes from other continental shelf systems (Fennel et al. 2009).

Sediment-water O_2 fluxes were highly correlated with bottom-water O_2 concentrations (Fig. 5), consistent with the mechanistic description of O_2 flux magnitude being dependent on O_2 concentration (Cai and Sayles 1996). Square-root dependence between O_2 flux and bottom-water O_2 concentration has been hypothesized (Bouldin 1968) and shown to fit fine-scale porewater O_2 profiles (Cai and Sayles 1996). However, a non-linear regression using a square-root function provided a poorer fit ($R^2 = 0.21$) than did the linear fit shown in Fig. 5.

The sediment O_2 fluxes from this study were compared to those measured by Murrell and Lehrter (2011) to assess how different core handling and O_2 measurements influenced the calculated flux values. The average (±SE) O_2 flux for the present study was −8.7 (±1.8) mmol O_2 m^{-2} $day^{-1}$and was not statistically different than the average O_2 flux of −12.3 (±2.6) mmol m^{-2} day^{-1} from Murrell and Lehrter (2011). Reported O_2 fluxes from this shelf are similar to those reported from other continental shelf environments (Devol and Christensen 1993; Devol et al. 1997; Laursen and Seitzinger 2002).

N, P, and Si fluxes

Sediment NH_4^+ fluxes (Table 2) were similar to previous measurements for the Louisiana shelf. Rowe et al. (2002) reported NH_4^+ fluxes that ranged from 0.8 to 4.4 mmol m^{-2} day^{-1}, Morse and Rowe (1999) observed NH_4^+ fluxes beneath the plume ranging from 2.6 to 4.2 mmol m^{-2} day^{-1} [though these data appear to be a subset of the Rowe et al. (2002) data set], and Gardner et al. (1993) measured NH_4^+ fluxes ranging from 0.3 to 1.3 mmol m^{-2} day^{-1}. Sediment NO_3^- fluxes (Table 2) differed from those reported by Rowe et al. (2002) who observed only negative NO_3^- fluxes (range = −2 to −0.2 mmol m^{-2} day^{-1}), but were similar to the NO_3^- fluxes observed by Gardner et al. (1993); range −0.6 to 0.3 mmol m^{-2}−day^{-1}.

Sediment DIP fluxes (Table 2) were similar to the DIP fluxes previously reported for the Louisiana shelf ranging from −0.41 to 0.26 mmol m^{-2}−day^{-1} (Miller-Way et al. 1994; Morse and Rowe 1999). The only previous Si fluxes reported for the Louisiana shelf averaged 6.6 mmol m^{-2} day^{-1} (Miller-Way et al. 1994), which was larger than the average rate observed in this study (1.7 mmol Si m^{-2} day^{-1}).

A model developed by Eldridge and Morse (2008) estimated that sediment nitrogen fluxes could supply 25–60% of the water-column phytoplankton nutrient demand on the Louisiana continental shelf. Observations from the present study (Table 3) indicated that sediment-water fluxes of dissolved inorganic nitrogen generally supplied <10% of water-column nitrogen demand. The potential percent contributions of sediment DIP fluxes to water-column phytoplankton

phosphorus demand were similarly small. However, in comparison to estimated sub-pycnocline nutrient demand by phytoplankton, sediment DIN, DIP, and Si fluxes could potentially supply a large percentage of the demand (Table 3). Thus, sediment nutrient fluxes were potentially important for primary production occurring beneath the pycnocline, which has been shown to be a significant fraction of water-column primary production across much of the shelf (Lehrter et al. 2009).

Denitrification

Site average denitrification rates ranged from 0.9 to 2.8 mmol N m^{-2} day^{-1} and were similar to previously published denitrification rates for this system. Gardner et al. (1993) reported rates of 0.5–1.1 mmol N m^{-2} day^{-1}, but these observations were limited to one cruise in July of 1990 and were estimated indirectly based on stoichiometry of dissolved inorganic nitrogen and oxygen fluxes . Fennel et al. (2009) provided denitrification rates from the Louisiana shelf, measured by Gardner and McCarthy (unpublished) in October 2006, that averaged 2.0 (SE = 0.3) mmol N m^{-2} day^{-1}.

There have been only a few other studies of denitrification on the continental shelf using the N_2 flux method. The average denitrification rates obtained from the Arctic shelf (Devol et al. 1997), Massachusetts Bay (Nowicki et al. 1997), and the mid-Atlantic Bight (Laursen and Seitzinger 2002) ranged from 1.3 to 1.7 mmol N m^{-2} day^{-1}, similar to the average rate of 1.4 (SE = 0.08) determined in this study. On the Washington shelf, higher denitrification rates (average = 3.2 mmol N m^{-2} day^{-1}) were observed (Devol and Christensen 1993). More recently, denitrification measured from a depth range of 50–100 m in the Irish Sea region of the north Atlantic shelf averaged 0.1 mmol N m^{-2} day^{-1} (Trimmer and Nicholls 2009), whereas rates measured in the Baltic Sea in the same depth range as for the sites reported herein ranged from 0.1 to 0.5 mmol N m^{-2} day^{-1} (Deutsch et al. 2010). The latter two studies both used the isotope-pairing method to estimate denitrification (Nielsen 1992). In a comparison of the isotope-pairing method with the N_2:Ar flux method, the isotope-pairing method was found to significantly underestimate the denitrification rate observed directly with the N_2 flux method (Ferguson and Eyre 2007). Ferguson and Eyre (2007) identify a need for more method comparison studies, across a range of environmental conditions. Such studies are needed to assess whether differences in denitrification rates are attributable to environmental differences or to methodological differences.

The N_2 flux rates presented offer a means to evaluate the role of denitrification as a nitrogen sink. If the average denitrification rate of 1.4 mmol N m^{-2} day^{-1} is assumed to be representative of the shelf, a first order estimate of the denitrification sink may be calculated. Assuming the 200 meter bathymetry contour as the seaward boundary of the continental shelf (Seitzinger et al. 2006), the area of the Louisiana shelf is estimated to be 65,910 km^2. Hence, shelf-wide denitrification would be on the order of 2.8×10^9 mol N per month. Given an estimated mean N load of 7.0×10^9 mol N per month delivered directly to the shelf from the Mississippi River for the months March to September (1968–2007), the denitrification sink would account for 39% (SE = 5%, estimated by error propagation) of this load. These results are comparable to estimates for other shelf systems where nitrogen sinks through denitrification have been estimated to account for 30–60% of nitrogen loads (Seitzinger et al. 2006; Deutsch et al. 2010).

NO_3^- fluxes strongly covaried with O_2 concentrations (Fig. 5) and were observed to have a complex, multi-variable relationship with bottom-water O_2 concentration, NH_4^+ flux, and N_2 flux (Fig. 6). The largest NO_3^- flux out of the sediments (Table 2) occurred at Z04 during March 2005 where the bottom-water O_2 concentration (141 mmol m^{-3}) was among the highest observed. This large NO_3^- flux coincided with the largest N_2 flux and among the smallest NH_4^+ fluxes observed (Table 2). The largest NO_3^- flux into the sediments occurred at Z02 in June 2006 and coincided with the lowest bottom-water O_2 concentration (12 mmol m^{-3}) and among the highest observed NO_3^- concentrations (8.6 mmol m^{-3}). A large NH_4^+ flux and a small N_2 flux were also observed at this site in June 2006 and suggested that under these low O_2 conditions coupled nitrification–denitrification was inhibited and that uptake of NO_3^- may have been largely driven by dissimilatory nitrate reduction to ammonia or DNRA (McCarthy et al. 2008).

Because most sites were not O_2 depleted in this study, denitrification appeared to proceed primarily

through coupled nitrification–denitrification. Evidence for coupled nitrification–denitrification included the positive relationships between bottom-water O_2 concentration and NO_3^- flux (Fig. 5) and between NO_3^- flux and N_2 flux ($r = 0.54$, $P = 0.02$). The lack of an observed relationship between bottom-water NO_3^- concentration and denitrification was consistent with previous observations indicating that coupled nitrification–denitrification was the dominant pathway (>90%) for denitrification when bottom-water NO_3^- concentrations were less than 10 mmol m^{-3} (Seitzinger et al. 2006), as it was at most sites in this study (Table 1). Bottom-water O_2 concentrations must be sufficient for coupled nitrification–denitrification to occur, and the results suggested that hypoxic bottom waters reduced coupled nitrification–denitrification and thereby increased NH_4^+ efflux from the sediment. Similar, hypoxia-induced patterns of sediment-water nitrogen fluxes have been reported from a number of coastal systems (reviewed by Middelburg and Levin 2009).

There was not a significant relationship between sediment O_2 flux and N_2 flux as has been observed in other analyses (Fennel et al. 2009). This may be due to the lower range of rates for O_2 (Fig. 4) and N_2 (Table 2) observed in this study as compared to the ranges of O_2 and denitrification rates, 0 to −95 mmol O_2 m^{-2} day^{-1} and 0 to 10 mmol N m^{-2} day^{-1}, respectively, reported in Fig. 4 of Fennel et al. (2009). Further, the Fennel et al. (2009) dataset did not contain any sites with O_2 concentrations less than 63 mmol m^{-3}, whereas in the present dataset 33% of the stations had O_2 concentrations that were hypoxic (ranging from 12 to 62 mmol m^{-3}). The interactions observed between bottom-water O_2 concentrations and flux rates (Figs. 5, 6) indicate that a linear paramterization of denitrification as a function of O_2 flux may be too simplistic for this environment.

Other modeling exercises have determined that denitrification was sensitive to the organic matter sedimentation rate and bottom-water concentrations of O_2 and nitrate (Middelburg et al. 1996). In the current study, it was not possible to estimate the sedimentation rate. Though, empirical relationships observed between water-column chl*a* and both DIC and N_2 flux rates (data not shown), indicated the potential coupling between labile organic matter in the water-column and sediment-water flux rates. Further, the lack of a relationship between sediment organic matter concentrations (Table 1) and any of the flux rates suggested that organic matter quality was more important than quantity. A similar conclusion was inferred for the sediments of the mid-Atlantic bight (Laursen and Seitzinger 2002). In sum, there is still much uncertainty about the controls of denitrification on this shelf, but O_2 concentrations appear to be a primary determinant of nitrification/denitrification rates (Childs et al. 2002). Hence, hypoxia may act as a positive feeback to eutrophication by reducing nitrification/denitrification and, in turn, increasing the release of NH_4^+ from the sediments.

Zones of similarity

Empirical relationships between MR nutrient loads and hypoxic area explain 50–60% of the variability in mid-summer hypoxia area, but regression model predictions of the amount of nutrient reductions required to meet the management goal of an average hypoxic area of 5,000 km^2 have high uncertainty (Greene et al. 2009). To reduce uncertainties in model predictions, representative hydrodynamic-eutrophication models are being developed. However, in the mechanistic sense there is high uncertainty about many of the physical transport and biogeochemical processes that are required to be modeled to accurately represent the development of hypoxia. This is especially true for sediment-water exchanges for which there have been few measurements. Identification of zones of similar sediment-water flux characteristics would reduce some of the modeling uncertainty associated with parameterizing initial and boundary conditions for the sediments.

The conceptual schemes proposed by Rowe and Chapman (2002) and Dale et al. (2010) included some hypothesized spatial patterns that may be evaluated with data collected from this study. Rowe and Chapman (2002) hypothesized that the sediment respiration in zone 1 would be primarily anaerobic owing to the high sedimentation rates from the plume and an abundance of oxidized iron and manganese that could be used as electron acceptors. They suggested aerobic and anaerobic metabolism would be balanced, i.e. O_2 uptake would be equivalent to DIC release from the sediments, in zone 2 as long as O_2 was present. In zone 3 it was hypothesized that O_2 concentration in the bottom-water would be sufficient

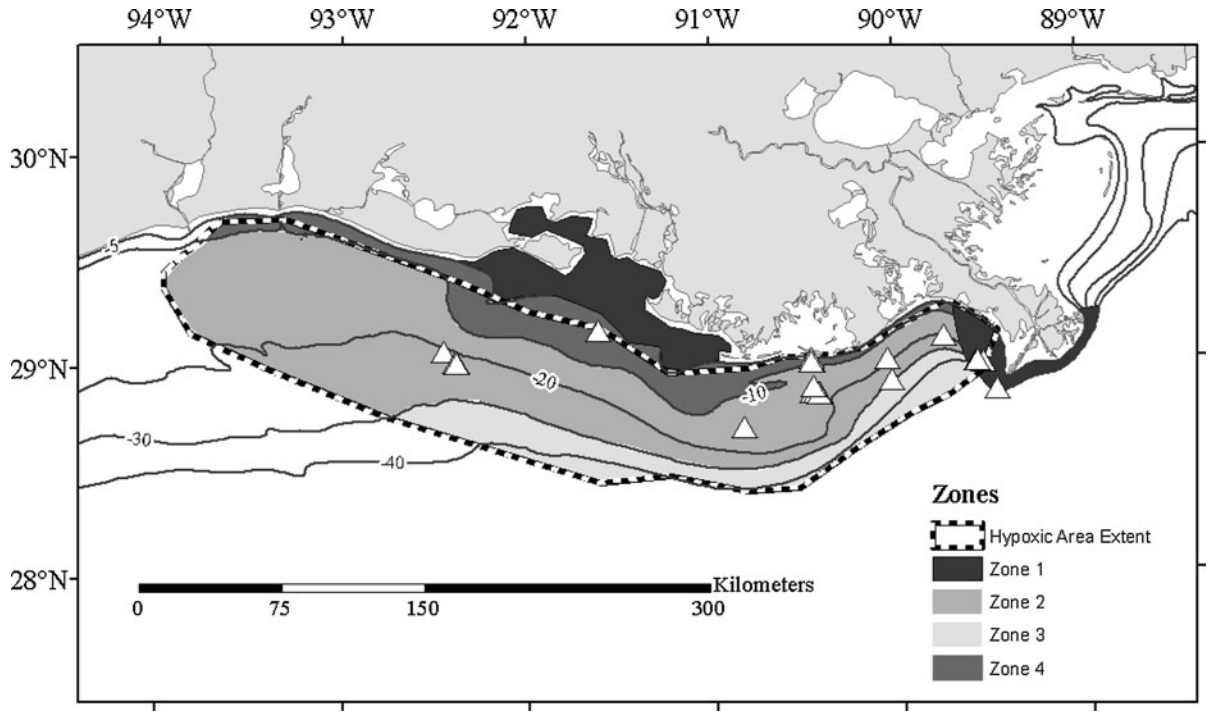

Fig. 8 A revision to the four zones of similarity within the maximal hypoxic area extent (region enclosed by the *dashed black* and *white line*, area = 29,130 km^2, digitized from Rabalais et al. 2002). In the plume area west of the birdsfoot delta, zone 1 transitions to zones 2 and 3 similar to the salinity contours observed in Fig. 1. The zone 1 area south of the passes for the Atchafalaya River extends to the 5 m contour. The zone 4 area is drawn with the boundaries being the 5 and 10 m contours. Zone 2 occupies the area between the 10 and 30 m contours. Zone 3 occupies the depths > 30 m to the extent of the polygon outlining the maximal hypoxic area extent. *Triangles* are the locations where sediments fluxes were measured in this study

to maintain elevated rates of aerobic versus anaerobic respiration. In the present study, the DIC flux rates were generally greater than the O_2 flux rates (Fig. 4). These results indicated that anaerobic processes were dominant in these sediments. Thus, realistic models of sediment O_2 dynamics for this shelf will need to include the accumulation of oxygen debt from reduced nitrogen, iron, managanese, and sulfur.

Rowe and Chapman (2002) hypothesized that primary production rates would be highest in zone 2 owing to alleviation of light limitation and abundant nutrients in this region. However, results presented in Fig. 7 indicated that Z01 and Z04 had higher primary production than Z02 and Z03. Spatial patterns in euphotic zone chl*a* concentrations mirrored the patterns observed in primary production with elevated values observed at Z01 and Z04 and lower values at Z02 and Z03.

Dale et al. (2010) hypothesized that zone 2 sub-pycnocline respiration would be dominated by water-column respiration while zone 3 sub-pycnocline respiration would be dominated by the sediments. Across the shelf, sediment metabolism was previously estimated to be the dominant respiratory pathway beneath the pycnocline, on average accounting for 75% of the respiration (Dortch et al. 1994; Quiñones-Rivera et al. 2007). However, a recent study based on sediment-water O_2 flux measurements and water-column measurements of oxygen demand below the pycnocline found that sediments were responsible for $20 \pm 4\%$ of the sub-pycnocline respiration (Murrell and Lehrter 2011). In the present study it was observed that O_2 fluxes were often small compared to DIC fluxes (Fig. 4). Recalculation of the sediment contribution to sub-pycnocline respiration using these DIC exchange rates yielded sediment respiration contributing 19–31% of the sub-pycnocline respiration (sediments + water-column, assumed a water-column respiration stoichiometry of DIC/O_2 = 1). Some of the variation in the percent

contributed by sediments could be attributed to differences in the thickness of the bottom-water layers (e.g. Fig. 3). At smaller sub-pynocline water depths, the relative contribution of the sediments was greater. The average thickness of the water-column below the pycnocline was 12, 9, 8, and 4 m at Z01, Z02, Z03, and Z04, respectively.

An updated conceptual model of the role of the sediments in system metabolism on the Louisiana continental shelf

The spatial patterns observed in salinity data (Fig. 1), sediment respiration (Fig. 4), and primary production (Fig. 7) indicated that the greatest variability in hydrography and metabolism on the shelf existed in an inshore to offshore, or north to south, gradient. Only in the lower Mississippi plume region did the salinity gradient orient itself in an east to west direction (Fig. 1). As such, we have redrawn the zones of similarity (Fig. 8). The new conceptual model has 4 zones, but the zonal scheme differs from Dale et al. (2010) in that the zones are expanded to the maximal extent of the hypoxic zone and the gradients are oriented in a north to south direction. In Fig. 8, the 5, 10, and 30 m bathymetry contours are used as features to delineate the zones. Based on how the stations from this study map against the zones in Fig. 8, we propose that zones 1 and 4 will have sediment-water flux and water-column production rates similar to sites Z01 and Z04, respectively. The new zone 2 encompasses site Z02 and Z03, based on similarities between these sites, and, thus, may be characterized by the results presented for these sites. The new zone 3 is envisioned as an oligotrophic region, similar to the original concept, but is displaced further to the south at depths > 30 m. None of the sites in the present study occupied the new zone 3. This refinement of the zonal model provides a new spatial scaling scheme for estimating the significance of sediment-water fluxes in the hypoxic region. Further measurements of sediment-water fluxes along inshore to offshore transects are needed to validate this zonal scheme.

In summary, three relationships were observed for the shelf that had previously been inferred. (1) Changes in bottom-water O_2 concentrations strongly affected the magnitude and direction of nitrogen fluxes. This has important implications for feedbacks between increased nutrient loading, hypoxia, and the manner in which the shelf processes nutrients. (2) Observed N_2 flux rates indicated that denitrification was a major nitrogen sink. (3) Sediment nutrient fluxes were generally small percentages of total water-column phytoplankton nutrient demand, though sediments could be important nutrient sources for sub-pycnocline primary production. These observations constrain the potential role of sediments in carbon, oxygen, and nutrient dynamics and will be useful in the development of mechanistic models for simulating shelf hypoxia.

Acknowledgments We thank A. Almario, J. Aukamp, M. Barron, J. Campbell, G. Craven, L. Oliver, R. Quarles, J. Scott, and R. Stanley for assistance in the collection and analysis of sediment samples. We thank J. Cornwell and M. Owens for analyzing N_2, O_2, and Ar samples from several of the early cruises. We thank the US EPA Office of Water and Gulf of Mexico Program Office for their support of ship time, and the crews of the OSV *Bold* and the R/V *Longhorn* which made this work possible. We thank C. Peacher, P. Caraballo, D. Bullock, and the facilties' staff for designing and building the sediment incubation systems, and for all the other facilities support for this work. Critical reviews by R. Greene, W. Gardner, J. Melack and three anonymous reviewers greatly improved this manuscript. We dedicate this contribution to the memory of our friend and EPA colleague R.L. Quarles. This study was funded, reviewed, and approved for publication by the US EPA, National Health and Environmental Effects Research Laboratory; however, the contents are solely the views of the authors. Use of trade names or commercial products does not constitute endorsement by the US EPA. Contribution number 1373 from the US EPA, Gulf Ecology Division.

References

Aller JY, Aller RC (1986) Evidence for localized enhancement of biological activity associated with tube and burrow structures in deep-sea sediment at the HEBBLE site, western North Atlantic. Deep-Sea Res I 33:755–790

Aller RC, Blair NE, Xia Q, Rude PD (1996) Remineralization rates, recycling, and storage of carbon in Amazon shelf sediments. Cont Shelf Res 16:753–786

American Public Health Association (APHA) (1989) Standard methods for the examination of water and wastewater, 17th Edition. American Public Health Association. Washington, D.C

Aspila KI, Agemain H, Chau ASY (1976) A semi-automated method for the determination of inorganic and total phosphate in sediments. Analyst 101:187–197

Aulenbach BT, Buxton HT, Battaglin WT, Coupe RH (2007) Streamflow and nutrient fluxes of the Mississippi-Atchafalaya River Basin and subbasins for the period of record through 2005: U.S. Geological Survey Open-File Report 2007–1080

Bianchi TS, DiMarco SF, Cowan JH, Hetland RD, Chapman P, Day JW, Allison MA (2010) The science of hypoxia in the Northern Gulf of Mexico: a review. Sci Total Environ 408:1471–1484

Bouldin DR (1968) Models for describing the diffusion of oxygen and other mobile constituents across the mud-water interface. J Ecol 56:77–87

Cai W-J, Sayles FL (1996) Oxygen penetration depths and fluxes in marine sediments. Mar Chem 52:123–131

Childs CR, Rabalais NN, Turner RE, Proctor LM (2002) Sediment denitrification in the Gulf of Mexico zone of hypoxia. Mar Ecol Prog Ser 240:285–290

Cook PLM, Wenzöfer F, Glud RN, Huettel M (2007) Benthic solute exchange and carbon mineralization in two shallow subtidal sandy sediments: impact of advective porewater exchange. Limnol Oceanogr 52:1943–1963

Cowan JLW, Boynton WR (1996) Sediment-water oxygen and nutrient exchanges along the longitudinal axis of Chesapeake Bay: seasonal patterns, controlling factors and ecological significance. Estuaries 19:562–580

Dagg MJ, Ammerman JW, Amon RMW, Gardner WS, Green RE, Lohrenz SE (2007) A review of water column processes influencing hypoxia in the northern Gulf of Mexico. Estuar Coasts 30:735–752

Dale VH, Kling CL, Meyer JL, Sanders J, Stallworth H, Armitage T, Wangsness D, Bianchi TS, Blumberg A, Boynton W (2010) Hypoxia in the Northern Gulf of Mexico. Springer-Verlag Inc, New York

Deutsch B, Forster S, Wilhelm M, Dippner JW, Voss M (2010) Denitrification in sediments as a major sink in the Baltic Sea: an extrapolation using sediment characteristics. Biogeosciences 7:3259–3271

Devol AH, Christensen JP (1993) Benthic fluxes and nitrogen cycling in sediments of the continental margin of the eastern North Pacific. J Mar Res 51:345–372

Devol AH, Codispoti LA, Christensen JP (1997) Summer and winter denitrification rates in western arctic shelf sediments. Cont Shelf Res 17:1029–1050

Diaz RJ, Rosenberg R (2008) Spreading dead zones and the consequences for marine ecosystems. Science 321:926–929

Dortch Q, Rabalais N, Turner RE, Rowe GT (1994) Respiration rates and hypoxia on the Louisiana shelf. Estuaries 17:862–872

Eldridge PM, Morse JW (2008) Origins and temporal scales of hypoxia on the Louisiana shelf: Importance of benthic and sub-pycnocline water metabolism. Mar Chem 108:159–171

Fennel K, Brady D, DiToro D, Fulweiler RW, Gardner WS, Giblin A, McCarthy MJ, Rao A, Seitzinger S, Thouvenot-Korppoo M, Tobias C (2009) Modeling denitrification in aquatic sediments. Biogeochemistry 93:159–178

Ferguson AJP, Eyre BD (2007) Seasonal discrepancies in denitrification measured by isotope pairing and N2:Ar techniques. Mar Ecol Prog Ser 350:19–27

Gardner WS, Escobar Briones E, Cruz Kaegi E, Rowe GT (1993) Ammonium excretion by benthic invertebrates and sediment-water nitrogen flux in the Gulf of Mexico near the Mississippi River outflow. Estuaries 16:799–808

Glud RN (2008) Oxygen dynamics of marine sediments. Marine Biology Research 4:243–289

Glud RN, Blackburn N (2002) The effects of chamber size on benthic oxygen uptake measurements: a simulation study. Ophelia 56:23–31

Glud RN, Berg P, Fossing H, Jørgensen BB (2007) Effect of the diffusive boundary layer (DBL) on the benthic mineralization of O_2 distribution: a theoretical modeling exercise. Limnol Oceanogr 52:547–557

Goñi MA, Gordon ES, Monacci NM, Clinton R, Gisewhite R, Allison MA, Kineke G (2006) The effect of Hurricane Lili on the distribution of organic matter along the inner Louisiana shelf (Gulf of Mexico, USA). Cont Shelf Res 26:2260–2280

Green RE, Bianchi T, Dagg MJ, Walker ND, Breed GA (2006) An organic carbon budget for the Mississippi River turbidity plume and plume contributions to air-sea CO_2 fluxes and bottom water hypoxia. Estuar Coasts 29:579–597

Greene RM, Lehrter JC, Hagy JD (2009) Multiple regression models for hindcasting and forecasting midsummer hypoxia in the Gulf of Mexico. Ecol Appl 19:1161–1175

Holmes RM, Aminot A, Kerouel R, Hooker B, Peterson BJ (1999) A simple and precise method for measuring ammonium in marine and freshwater ecosystems. Can J Fish Aquat Sci 56:1801–1808

Hopkinson CS Jr, Smith EM (2005) Estuarine respiration: an overview of benthic, pelagic. and whole system respiration. Oxford University Press, Oxford

Huettel M, Webster IT (2001) Porewater flow in permeable sediments. In: Boudreau B, Jörgensen BB (eds) The Benthic boundary bayer. New York, Oxford University Press, pp 144–179

Jørgensen BB (1982) Mineralization of organic matter in the sea bed—the role of sulfate reduction. Nature 296: 643–645

Kana TM, Darkangelo C, Hunt MD, Oldham JB, Bennett GE, Cornwell JC (1994) Membrane inlet mass spectrometer for rapid high-precision determination of N_2, O_2, and Ar in environmental water samples. Anal Chem 66: 4166–4170

Laursen AE, Seitzinger SP (2002) The role of denitrification in nitrogen removal and carbon mineralization in Mid-Atlantic Bight sediments. Cont Shelf Res 22:1397–1416

Lehrter JC, Murrell MC, Kurtz JC (2009) Interactions between freshwater input, light, and phytoplankton dynamics on the Louisiana continental shelf. Cont Shelf Res 29:1861–1872

McCarthy MJ, McNeal KS, Morse JW, Gardner WS (2008) Bottom water hypoxia effects on sediment-water interface nitrogen transformations is a seasonally hypoxic, shallow bay (Corpus Christi Bay, TX, USA). Estuar Coasts 31:521–531

Middelburg JJ, Levin LA (2009) Coastal hypoxia and sediment biogeochemistry. Biogeosciences 6:1273–1293

Middelburg JJ, Soetart K, Herman PMJ, Heip C (1996) Denitrification in marine sediments: a model study. Global Biogeochem Cycles 10:661–673

Miller-Way T, Boland GS, Rowe GT, Twilley RR (1994) Sediment oxygen consumption and benthic nutrient fluxes on the Louisiana continental shelf: a methodological comparison. Estuaries 17:809–815

Morse JW, Rowe GT (1999) Benthic biogeochemistry beneath the Mississippi River plume. Estuaries 22:206–214

Murrell MC, Lehrter JC (2011) Sediment and lower water-column respiration in the seasonal hypoxic region of the Louisiana continental shelf. Estuar Coasts. doi: 10.1007/s12237-010-9351-9

Nielsen LP (1992) Denitrifcation in sediments determined from nitrogen isotope pairing. FEMS Microbiol Ecol 86: 357–362

Nowicki BL, Requintina E, van Keuren D, Kelly JR (1997) Nitrogen losses through sediment denitrification in Boston Harbor and Massachusetts Bay. Estuaries 20:626–639

Pelegri S, Nielsen LP, Blackburn TH (1994) Denitrification in estuarine sediment stimulated by the irrigation activity of the amphipod *Corphium volutator*. Mar Ecol Prog Ser 105:285–290

Quiñones-Rivera Z, Wissel B, Justic D, Fry B (2007) Partitioning oxygen sources and sinks in a stratified, eutrophic coastal ecosystem using stable oxygen isotopes. Mar Ecol Prog Ser 342:69–83

Rabalais NN, Turner RE, Scavia D (2002) Beyond science into policy: Gulf of Mexico hypoxia and the Mississippi River. Bioscience 52:129–142

Rabalais NN, Turner RE, Gupta BK, Boesch DF, Chapman P, Murrell MC (2007) Hypoxia in the northern Gulf of Mexico: does the science support the plan to reduce, mitigate, and control hypoxia? Estuar Coasts 30:753–772

Roden EE, Edmonds JW (1997) Phosphate mobilization in iron-rich anaerobic sediments: microbial Fe(III) oxide reduction vs. iron-sulfide formation. Archiv für Hydrobiol 139:347–378

Rowe GT, Chapman P (2002) Continental shelf hypoxia: some nagging questions. Gulf Mexico Sci 2:153–160

Rowe GT, Cruz Kaegi ME, Morse JW, Boland GS, Escobar Briones EG (2002) Sediment community metabolism associated with continental shelf hypoxia, northern Gulf of Mexico. Estuaries 25:1106–1907

Røy H, Hüttel M, Jørgensen BB (2005) The influence of topography on the functional exchange surface of marine soft sediments, assessed from sediment topography measured in situ. Limnol Oceanogr 50:106–112

Sampere TP, Bianchi TS, Wakeham SG, Allison MA (2008) Sources of organic matter in surface sediments of the Louisiana Continental margin: effects of major depositional/transport pathways and Hurricane Ivan. Cont Shelf Res 28:2472–2487

Sampou P, Oviatt CA (1991) A carbon budget for a eutrophic marine ecosystem and the role of sulfur metabolism in sedimentary carbon, oxygen and energy dynamics. J Mar Res 49:825–844

Seitzinger S, Harrison JA, Bohlke JK, Bouwman AF, Lowrance R, Peterson B, Tobias C, Van Drecht G (2006) Denitrification across landscapes and waterscapes: a synthesis. Ecol Appl 16:2064–2090

Trimmer M, Nicholls JC (2009) Production of nitrogen gas via anammox and denitrification in intact sediment cores along a continental shelf to slope transect in the North Atlantic. Limnol Oceanogr 54:577–589

Walker ND, Hammack AB (2000) Impacts of winter storms on circulation and sediment transport: Atchafalaya-Vermilion Bay region, Louisiana, USA. J Coastal Res 16:996–1010

Welschmeyer NA (1994) Fluormetric analysis of chlorophyll a in the presence of chlorophyll b and phaeopigments. Limnol Oceanogr 39:1985–1992

Wiseman WJ, Rabalais NN, Turner RE, Dinnel SP, MacNaughton A (1997) Seasonal and interannual variability within the Louisiana coastal current: stratification and hypoxia. J Mar Syst 12:237–248